ELSEVIER

Physica C 377 (2002) 156–164

PHYSICA C

www.elsevier.com/locate/physc

Magnetization and AC loss in a superconductor with an elliptical cross-section and arbitrary aspect ratio

Bennie ten Haken *, Jan-Jaap Rabbers, Herman H.J. ten Kate

Department of Applied Physics, Low Temperature Division, University of Twente, P.O. Box 217, 7500 AE Enschede, The Netherlands

Received 21 August 2001; received in revised form 9 October 2001; accepted 24 October 2001

Abstract

An analytical approximation is developed for the magnetization of an infinitely long superconductor with an elliptical transverse cross-section. The superconductor is modeled in the critical state with a critical current density that is not dependent on the magnetic field. The aspect ratio of the ellipse is varied from one (= circle) to infinitely large. The magnetic field is applied perpendicular or parallel to the broadest face. The analytical expression is compared with a more detailed model that utilizes a numerically optimized contour for the boundary of the saturated zone. The two methods are compared and the maximum error is estimated at 2% for the optimized contour approach and 5% for the analytical approximation. The analytical model is compared with a magnetization loss measurement on a high-T_c superconducting tape with an aspect ratio of nearly 20. A good agreement is obtained for a magnetic field pointing perpendicular as well as parallel to the broadest face of the tape. An interesting result for the magnetic behavior determined for the ellipse is that it contradicts with the behavior that is predicted for an infinitely thin strip in perpendicular field. The difference is attributed to the two specific assumptions made in the thin strip model: the constant critical current density distribution across the tape and the magnetic-field profile that does not exclude unsaturated currents in the shielded zone.

PACS: 74.25.Ha; 74.76.−w; 85.25.Kx
Keywords: AC loss; Magnetization; Critical state model; Bi-based cuprates

1. Introduction

A significant part of the energy loss in superconductors in technical applications is caused by the magnetization loss. The typical voltage current relation of a superconductor leads to a hysteretic magnetization curve. The magnetization loss due to this hysteresis can be modeled with an analytical expression in some specific cases. The critical state model proposed by Bean assumes that the magnitude of the current density (J) is always equal to the critical current density (J_c) and that the sign of J is equal to the sign of the last non-zero electrical field that was present. According to this model the situation $J = 0$ only occurs in the (shielded) volume where the electrical field is kept equal to zero all the time [1].

* Corresponding author. Tel.: +31-53-489-3190; fax: +31-53-489-1099.
E-mail address: b.tenhaken@tn.utwente.nl (B. ten Haken).

0921-4534/01/$ - see front matter
PII: S0921-4534(01)01194-7

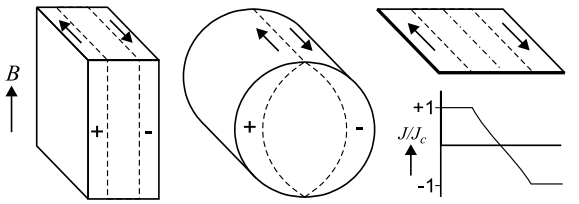

Fig. 1. Three geometries that have been evaluated with the critical state model: infinite slab in a parallel field (left), a cylinder in perpendicular field and an infinitely thin strip in perpendicular field (right). The graph J/J_c shows the current distribution along the strip, with $0 < |J| < J_c$ in the center.

Several specific geometries have been evaluated with the critical state model (see Fig. 1). The magnetization can be expressed exactly for an infinitely large slab with finite thickness in a parallel magnetic field [1]. The critical state approach is also applied to infinitely long structures with a various cross-sections. A very specific geometry that has been considered is the infinitely thin strip in perpendicular field, where analytical expressions are derived for the magnetization and the AC loss [2,3]. Conductors with circular and elliptical cross-sections have been analyzed in different styles [4–6]. This case can also be treated as a special case of the three dimensional ellipsoids [7,8].

For the magnetization of a circular cylinder in a perpendicular field analytical approximations have been presented. In these calculations the shape of the contour between the saturated area ($J = \pm J_c$) and the shielded area ($J = 0$) is described with an approximated expression [4,5]. Additionally there are many numerical models that have been developed to describe specific conductor geometries or deviations from the critical state, such as an arbitrary voltage current relation or a field dependent critical current density [9–14].

The development of high-T_c superconductors has increased the interest for the magnetic behavior of conductors with a high aspect ratio. $Bi_2Sr_2Ca_2Cu_3O_x$ tapes with a Ag matrix are produced as flat tapes with an aspect ratio typically between 15 and 20 [15]. For coated $YBa_2Cu_3O_x$ superconductors the aspect ratio of the superconducting cross-sectional area can be more than 1000 [16,17]. Despite all these new materials with a high aspect ratio the typical magnetic behavior predicted for an infinitely thin strip in a perpendicular field has not been experimentally verified yet. In particular in high-T_c tapes and coated conductors the predicted fourth power dependence for the loss in small perpendicular magnetic fields is not observed yet [18–22].

The materials development in high-T_c superconductors and the experimental results mentioned above call for a more dedicated description of the magnetization in a superconductor with a large aspect ratio in the range from 10 to 10^4. It is interesting to determine the aspect ratio that is required in order to obtain the typical magnetic behavior derived for an infinitely thin strip in a perpendicular field [2,3]. An important assumption in this thin strip model is that gradients in the perpendicular field are neglected across the thickness of the strip. This assumption leads to an averaged current density in the shielded central zone of the strip below the critical current density. In the critical state concept any current density $0 < |J| < J_c$ will always arrange itself in a very thin saturated layer at the surface of the conductor. In the articles that present the strip model it is argued the precise current profile within the thickness is not significant for the magnetic behavior and as a consequence the typical aspects of the strip model are attributed to the constant product of J_c and thickness over the width of the strip, similar as in a rectangular conductor.

In this study the magnetization of an infinitely long superconductor with an elliptical cross-section is investigated in the critical state. Particular attention is paid to the case of a high aspect ratio in perpendicular magnetic field in order to be able to describe the loss in high-T_c superconducting tapes and coated conductors. A new analytical approximation is developed that is based on the onset of the magnetization curve on one hand and the state at full penetration on the other hand.

This description is compared with a more detailed model with a numerically optimized contour for the saturated zone. The magnetization loss is calculated and verified with a dedicated experiment on a superconducting tape where the field dependence of J_c is suppressed by a DC background field. Finally the validity of the approximation for the elliptical shape and the existing

model for an infinitely thin strip is discussed for a high-T_c coated conductor with a finite thickness.

2. Analytical approximation

In the following approximate calculation an elliptical cross-section is considered with a physical width d and height $d\alpha$, so that the aspect ratio is α or $1/\alpha$. For the calculations a normalized coordinate system is used in which the ellipse has a width of 2 along the x-direction and a height 2α in the y-direction, which is also the direction for the applied magnetic field (see Fig. 2). First the magnetization (M) and the internal magnetic field (B) are calculated for a fully penetrated ellipse. The second step is to derive the slope of the magnetization curve $M(B)$ in the limit for small fields starting from the virgin state. These conditions are used as constrains for an approximation of the entire magnetization curve.

2.1. Full penetration

The penetration field of an ellipse is the magnetic field in the center pointing in the y-direction, when the two half sections are filled with a constant current density $J = \pm J_c$. The integral form of Biot–Savart for one quadrant determines the penetration field as

$$B_p(\alpha) = \frac{\mu_0 J_c d}{\pi} \int_0^{\alpha} \int_0^{x_b} \frac{x}{x^2 + y^2} \mathrm{d}x\,\mathrm{d}y, \qquad x_b = \sqrt{1 - (y/\alpha)^2}, \tag{1}$$

where x_b defines the outline of the ellipse in normalized units. The integration results in a shape factor that depends only on the aspect ratio:

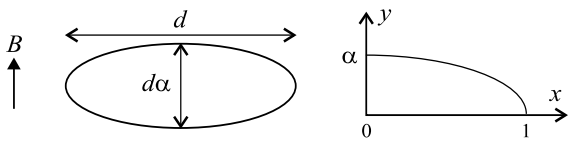

Fig. 2. The geometry of the ellipse, the direction of the applied field and the definition of the normalized coordinate system.

$$\frac{B_p(\alpha)}{B_{p,c}} = \frac{\alpha}{\sqrt{\alpha^2 - 1}} \arctan\sqrt{\alpha^2 - 1} = \frac{\alpha}{2\sqrt{1 - \alpha^2}} \ln\left(\frac{1 + \sqrt{1 - \alpha^2}}{1 - \sqrt{1 - \alpha^2}}\right)$$

and

$$B_{p,c} = \frac{\mu_0 J_c d}{\pi}. \tag{2}$$

This shape factor is exactly one for $\alpha = 1$, showing that $B_{p,c}$ represents the penetration field in a circle. For an infinitely large ellipse in parallel field ($\alpha = \infty$) the shape factor is $\pi/2$ and the penetration field is equal to the B_p of a slab in parallel field. The second formulation of the shape factor avoids imaginary intermediate results for $\alpha < 1$. The magnetization in a fully penetrated ellipse is

$$M_p = \frac{2 J_c d}{\pi \alpha} \int_0^{\alpha} \int_0^{x_b} x\,\mathrm{d}x\,\mathrm{d}y = \frac{2}{3\pi} J_c d. \tag{3}$$

Note that due to the rounded edges, the magnetization in the limit for large α is different from the magnetization in the infinite slab in parallel field.

2.2. Small applied field

For a circular cross-section a "$\cos(\theta)$" profile for the surface current is the well known solution to shield a homogenous external field perfectly, which can be generalized for an ellipse with arbitrary aspect ratio [4]. In an elliptical cross-section with an external field pointing in the y-direction, this is equal to a surface current at a position on the border $x = x_b$ that is proportionally to the value of this x-coordinate. The shielded magnetic field (B_s) in the center is then calculated as an integral over the outline x_b, where C represents the magnitude of the surface current and the path length in a section $\mathrm{d}y$ is $\mathrm{d}y/x_b$:

$$B_s(\alpha) = \frac{\mu_0 d}{\pi} \int_0^{\alpha} \frac{C x_b \cdot x_b}{x_b^2 + y^2} \frac{\mathrm{d}y}{x_b} = C \frac{\mu_0 d}{\pi} \int_0^{\alpha} \frac{\sqrt{1 - (y/\alpha)^2}}{1 - (y/\alpha)^2 + y^2} \mathrm{d}y,$$

$$B_s(\alpha) = C\frac{\mu_0 d}{2}\frac{\alpha}{1+\alpha}. \quad (4)$$

The magnetization for such a current profile is

$$M_s = \frac{2dC}{\pi\alpha}\int_0^{\alpha}\sqrt{1-(y/\alpha)^2}\,dy = C\frac{d}{2}. \quad (5)$$

When the two equations above are combined with $B_s = -B$ the slope dM/dB can be calculated exactly for an applied field, in the limit for small B. After a normalization in M and B the following result is obtained for the slope (m_0'):

$$b = \frac{B}{B_p(\alpha)}, \quad m = \frac{M}{M_p} \quad \text{and}$$
$$m_0' = -\frac{M_s B_p(\alpha)}{M_p B_s(\alpha)}$$
$$= -\frac{3}{2}\frac{\alpha+1}{\sqrt{\alpha^2-1}}\arctan\sqrt{\alpha^2-1}, \quad (6)$$

where the imaginary results for the root can be avoided with the substitution shown in the expression for the field of full penetration (Eq. (2)).

2.3. Approximated magnetization

The obtained results for the magnetization of an ellipse can be combined into a single expression for $m(b)$ in the following way:

$$m(b) = [(1-b)^{-m_0'} - 1] \quad \text{for } 0 \leqslant b \leqslant 1 \quad \text{and}$$
$$m(b) = -1 \quad \text{for } b > 1. \quad (7)$$

This expression satisfies the four constrains at $b = 0$ and 1:

$$m(0) = 0, \;\; m(0)' = m_0',$$
$$m(1) = -1 \;\text{ and }\; m(1)' = 0, \quad (8)$$

where m_0' is the only α dependent parameter. This analytical expression lacks a physical background for the exact shape in the intermediate regime. In the case of a circular cross-section where $m_0' = -3$ this method is presented earlier by Hartmann [10]. In an accurate comparison with a numerical model he shows that the absolute error in the normalized magnetization is smaller than 0.015 at $b = 0.5$.

3. Magnetization with an optimized contour

The analytical formulation for $m(b)$ presented above cannot be accepted as a precise approximation without a more detailed investigation of the magnetic properties of an elliptical superconductor. The magnetization of an elliptical cross-section is investigated in a more detailed approximation with the critical state model. The precise values for M and B are calculated by assuming a particular contour that separates the zone with $J = \pm J_c$ from the central zone where $J = 0$. The precise shape of the contour is determined by minimizing the shielded field numerically at selected positions in the cross-section, equivalent to a minimization of the Gibbs free energy [4,5]. This approach is expected to produce a more accurate result for extreme values of the aspect ratio (e.g. $\alpha \ll 1$), compared to the existing numerical methods that require a full and dense discretization of the cross-section.

3.1. The approximated current contour

A contour is defined that crosses the x-axis at $1-\beta$. In that case β represents the fraction of the conductor on the x-axis that is filled with current $(J = \pm J_c)$ and β can be defined as the penetration depth. The y-axis crossing is defined at $y = \alpha$, indicating that the contour always passes through the top center of the ellipse:

$$x_c(y) = \frac{[1-(y/\alpha)^2]^{1/p}(1-\beta^2)}{[1-(y/\alpha)^2]^{1/(2p)} + \beta}. \quad (9)$$

This formulation includes an exponent p that can be used as an additional degree of freedom to shape the contour $(0 < p \leqslant 1)$. The value of p is determined by the condition that the field at the center $(x = 0,\ y = 0)$ and at the edge of the penetrated zone $(x = 1-\beta,\ y = 0)$ are both exactly cancelled for all levels of penetration. Because of the symmetry in the y-direction the magnetic field in a point on the axis is expressed as

$$B(\alpha,x') = \frac{\mu_0 J_c}{\pi}\int_0^{\alpha}\left[\int_{-x_b}^{-x_c}\frac{-(x-x')}{(x-x')^2+y^2}\,dx + \int_{x_c}^{x_b}\frac{(x-x')}{(x-x')^2+y^2}\,dx\right]dy. \qquad (10)$$

The integration in x is done analytically and this result is used to evaluate the entire integral in a relatively fast procedure to determine the exponent p as function of the relative height and the level of penetration numerically. The obtained values for p are depicted in Fig. 3 and the shape of the contour for a wide range of aspect ratios is presented in Fig. 4.

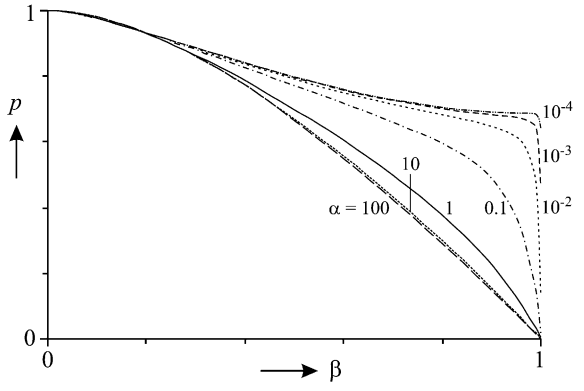

Fig. 3. The calculated values for the exponent p that determine the shape of the contour as function of the relative height α and the level of penetration β. The value for p is determined by minimizing the difference in field at $x = 0$ and $x = 1 - \beta$ on the x-axis numerically.

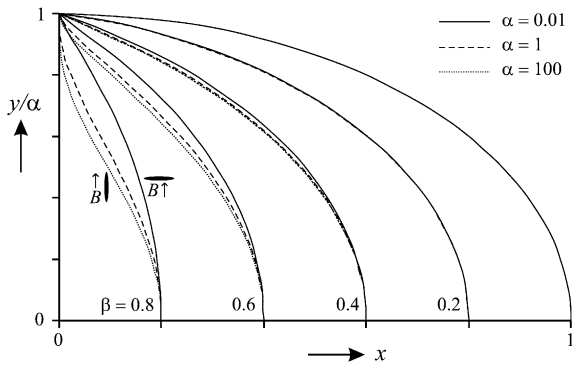

Fig. 4. The calculated shape of the contour at selected values for the penetration β and for three values of the relative height. The y-axis is normalized to the relative height.

The approximated contour shows some interesting features that can be discussed by considering the behavior of the exponent p that determines the precise shape of the contour near the y-axis. The largest dependence on the aspect ratio occurs for large values of the penetration. In Fig. 4 the contours are clearly separated for $\beta = 0.8$, where p ranges from 0.29 ($\alpha = 100$) to 0.68 ($\alpha = 1/100$). For a smaller value for the penetration ($\beta < 0.2$) the variation in the exponent is relatively small ($0.9 < p < 1$) and the dependence of the contour on the aspect ratio is therefore hardly visible.

3.2. Magnetization as a function of field

The current profiles that are derived in the optimized contour approximation are used to determine the magnetization curve $m(b)$ for different values of the aspect ratio. The integrals for the magnetic field in the center and the magnetization are calculated (partly) numerically for all levels of penetration ($0 \leqslant \beta \leqslant 1$). In Fig. 5 the magnetization curves obtained with the optimized contour are compared with the analytical expression that is presented earlier (Eq. (7)).

In general the resemblance between the different methods is very good for the entire range considered. The analytical expression correctly describes all the important features of the magnetization curve. The largest deviation is visible at $\alpha \geqslant 0.01$ and $m > 0.4$, where the analytical expression is

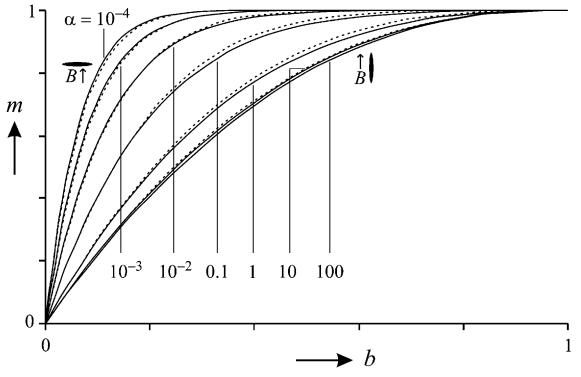

Fig. 5. The magnetization curves calculated with the analytical approximation (—) and with a numerically optimized contour (- - -) for different values of the relative height from $\alpha = 10^{-4}$ to 100.

slightly too large (maximum difference 2%) compared to the second order approximation. The largest error in m occurs in the limit for a very small relative height ($\alpha < 0.01$) where a negative difference (maximum 3%) occurs for small values of b and m. However, it can be stated that the differences between the two approximations are very small.

An interesting feature is the magnetic behavior for large aspect ratios ($\alpha \gg 1$ or $\alpha \ll 1$). Because of the numerical calculation of the field and magnetization integrals the optimization in p can lead to instable results in these two extreme cases. In the limit for large α the field on the x-axis becomes uniform for all levels of p. Therefore the numerical calculation of this exponent becomes inaccurate for $\alpha > 10^4$ in our case. However, because the condition of field homogeneity on the x-axis is already satisfied, an accurate result is obtained if the values for p, as derived for $\alpha = 100$, are used to calculate the $m(b)$ curve. In this limit the reduced magnetization is constant for all $\alpha > 100$. In the limit for small α the calculation of the field integral can lead to a numerical error. However, the value of the exponent p saturates in this limit for small α. In our case the accuracy of the result in m or b is not reduced if the values for p, as derived for $\alpha = 10^{-4}$, are used to calculate the $m(b)$ curve for all $\alpha < 10^{-4}$. Then the initial slope in $m(b)$ is a function of α according to the approximation for m_0' that is used in analytical expression (Eq. (7)).

3.3. Error approximation

For the error approximation it is important to consider the accuracy of the optimized contour approximation in detail. For this analysis we use the averaged absolute field error on the symmetry x-axis, in the zone where the magnetic field is shielded ($0 < x < 1 - \beta$). For a round wire this field error at $b = 0.5$ is 0.14% of the shielded field. This factor can be compared with numerical results on a round wire that are obtained relatively accurate already many years ago: $m(0.5) = -0.8603$ [10]. It appears that the error in m is only 0.08% in this case, which is nearly two times smaller than the average error in the shielded field on the symmetry axis. The field error in the shielded zone is calculated for all the considered aspect ratios. The maximum relative error occurs for small b and small α, in the limit for a small α this converges to 2%. Similar as in the round wire at $b = 0.5$ it is expected that the error in m is smaller than the average error in the shielded field. Therefore it is concluded that the error in m is smaller than 2% in the optimized contour approximation. Finally this results in an estimation for the relative error of 5% and the absolute error of 0.03 in the analytical expression for $m(b)$.

4. The AC loss

The normalized energy loss per cycle is directly calculated with the virgin $m(b)$ curve (see e.g. Ref. [10]):

$$q(b) = 4\int_0^b [m(b) - 2m(b')]\mathrm{d}b'. \tag{11}$$

This integral can be solved analytically for the approximation (Eq. 7) that is considered here:

$$q(b) = 4\left[\frac{2}{1-m_0'}\left((1-b)^{1-m_0'} - 1\right) + b\left((1-b)^{-m_0'} + 1\right)\right] \quad \text{for } 0 \leqslant b < 1, \tag{12a}$$

$$q(b) = 4\left[b - \frac{2}{1-m_0'}\right] \quad \text{for } b \geqslant 1. \tag{12b}$$

The reduced loss is expressed in physical units with:

$$Q(B) = M_\mathrm{p} B_\mathrm{p}(\alpha) q(b). \tag{13}$$

A useful formulation is the loss function (Γ) that determines the ratio of the energy loss in the considered volume and the energy contents of an identical volume in vacuum:

$$\Gamma(B) = \mu_0 \frac{Q(B)}{2B^2} = \mu_0 \frac{M_\mathrm{p}}{2B_\mathrm{p}(\alpha)} \frac{q(b)}{b^2} = \frac{1}{3}\frac{B_{\mathrm{p,c}}}{B_\mathrm{p}(\alpha)} \frac{q(b)}{b^2}. \tag{14}$$

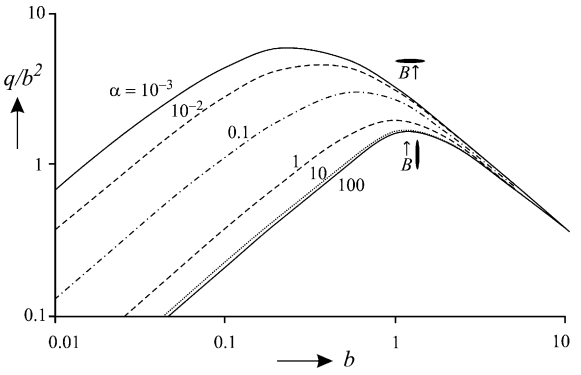

Fig. 6. The function $q(b)/b^2$ in the analytical approximation for different values of the relative height from $\alpha = 10^{-3}$ to 100.

The shape of the loss function can be considered with the function $q(b)/b^2$. The behavior of $q(b)/b^2$ is depicted in Fig. 6. Note that the normalization of b and q depends on the aspect ratio with $B_p(\alpha)$.

The shape of the function $q(b)/b^2$ for the analytical approximation shows several interesting features:

1. For a relative height equal or larger to one the shape of the loss function is in good agreement with the well-known behavior of a cylinder and an infinitely large slab in parallel fields. For $b \ll 1$ the slope in a double logarithmic plot is 1 ($q \propto b^3$) and for $b \gg 1$ the slope is -1 ($q \propto b$). However, due to the rounded edges the magnetization of an ellipse is always slightly different from a slab, even at full penetration.
2. For a small relative height ($\alpha \ll 1$) the shape of the function is only slightly changed compared to the circle. In particular it should be noted that the slope of 1 for $b \ll 1$ remains intact, also for very small values of the aspect ratio. In the limit for small fields it can be derived that $q = (2/3)m_0'(1 + m_0')b^3$ for all values of α.
3. The position of the peak in $q(b)/b^2$ is changed, for a small α it shifts to a lower value of b. This shift can be understood if the $m(b)$ curve of the cross-section is considered (see Fig. 3). The position of the largest curvature is shifted towards a lower value of b in this function too.
4. The maximum in $q(b)/b^2$ increases for a small relative height ($\alpha < 1$). This increase is due to the increase in the demagnetization factor, that represents the magnetized volume outside the considered cross-section.

4.1. The loss in physical units

Because of the aspect ratio dependence in the normalization of b and q it is interesting to consider the loss function Γ separately. In Fig. 7 an example is presented for a conductor with $J_c = 100$ A/mm^2 and a cross-sectional area determined by width $\times$ height is 1 mm^2.

For a large relative height ($\alpha \gg 1$) the loss curves translate towards smaller field values, compared to the loss function for a circle ($\alpha = 1$). This is due to the reduction of the penetration field proportional to the reduction of the width ($d \propto 1/\sqrt{\alpha}$, for a constant cross-sectional area). The magnitude of the maximum in the loss function is nearly constant for a large relative height.

For a small α the magnitude of the maximum in the loss function increases nearly proportional to $1/\alpha$, due to the increase of the demagnetization factor. The position of this maximum shifts towards a smaller B for a small α too. This typical behavior can be understood if the limiting cases for large and small field are considered. In the limit for small field and small aspect ratio the loss is proportional to $B^3/\alpha\sqrt{\alpha}$. For large B the loss is proportional to $B/\sqrt{\alpha}$ for all aspect ratios. The combination of these two dependencies leads to a

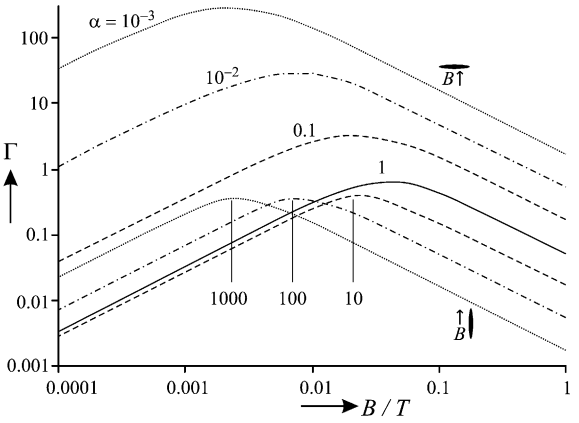

Fig. 7. The loss function Γ in the analytical approximation for a constant cross-sectional area ($d \times d\alpha = 1$ mm^2) with different values of the relative height $\alpha = 10^{-3}$ to 1000.

shift of the maximum in Γ that is proportional to $\sqrt{\alpha}$ for the smallest relative height.

Due to the typical behavior for large aspect ratios the maximum in Γ occurs at nearly the same position for a relative height of α and $1/\alpha$. This leads to the approximate relation: $\Gamma(1/\alpha) \approx \alpha\Gamma(\alpha)$, that is valid exactly for $B \gg B_p$ but is typically up to 50% wrong for small values of B. In an AC loss measurement this resembles a 90° rotation in the field, around the current axis of the sample.

5. Comparison with experimental results

A magnetization experiment is performed with a $Bi_2Sr_2Ca_2Cu_3O_x$ tape. The filamentary section in this tape sample is 3.36 mm wide and 0.174 high, which resembles an aspect ratio of 19.3. The critical current of the tape in self-field is 57 A at an electrical field of 10^{-4} V/m at 77 K. The AC loss is measured in a dipole set that can apply a magnetic field in any direction perpendicular to the current axis of the tape [23]. A common procedure is followed where the loss per cycle is measured in two directions of the magnetic field, parallel ($\alpha = 19.3$) and perpendicular ($\alpha = 1/19.3$) to the tape surface at 48 Hz and 77 K. At this frequency the (untwisted) filaments can be considered as fully coupled. A small DC magnetic field is applied in the direction perpendicular to the tape surface to investigate the role of the self-field, which influences the I_c that is measured with a transport current. The magnetization measurement is presented as the loss function Γ in Fig. 8 in combination with the analytical approximation, for both directions of the field.

A good agreement is observed with the discussed model if the loss is calculated with the geometrical dimensions and the measured I_c as listed above. The position of the peak in field level and magnitude closely agrees with the model. The largest deviation occurs in parallel field with no DC background field. In that case the deviation is significant at low fields (<10 mT). This deviation is attributed to the field dependence of J_c that is neglected in our model. It can be explained if the critical current density at 1 mT is approximately 2 times larger than in self-field with the I_c measurement. The loss measurement in a DC background field of 5 mT supports this explanation. At this level of the perpendicular DC field the loss is in better agreement with the critical state model and it is concluded that J_c is reduced to the same level as in the I_c measurement.

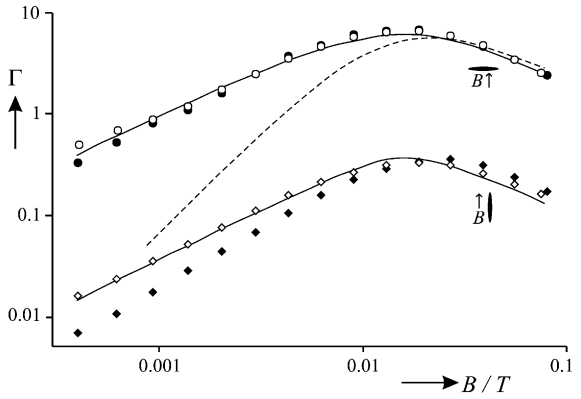

Fig. 8. The loss function $\Gamma(B)$ in a high-T_c tape measured for two directions of the field combined with the analytical approximation. The points with black markers are measured in an AC magnetic field only. The open symbols represent the points measured with a small DC background field of 5 mT in the perpendicular direction. The thin strip model in perpendicular field [2,3] is plotted with the dashed line.

The results of the elliptical model and the experimental results are in good agreement with each other for a typical superconducting tape. However, a significant disagreement is observed with the existing model for an infinitely thin strip in perpendicular field that predicts a loss proportional to B^4 for a small applied field. It could be stated that the aspect ratio of the tape is not sufficiently small to fulfill the condition of an infinitely thin strip or that the product of critical current density times thickness at the edges of the tapes is reduced. The model for the elliptical cross-section that is considered here does not predict such a B^4 behavior in the limit for small α. It is our expectation that the typical behavior of an infinitely thin strip will occur in a superconducting plane with a more distinct two-dimensional nature, where the superconducting current cannot be concentrated in a saturated layer on the surface (e.g. a small set of Cu–O layers). In the original papers [2,3] it is claimed that a constant current

density times thickness profile across the width is crucial for the typical behavior of the strip model. As a consequence it becomes more important to compare the magnetic behavior of the newest generation of high-T_c coated conductors accurately with the strip model and the model for a very thin ellipse as presented here.

6. Conclusion

The magnetization of a superconducting ellipse with an arbitrary aspect ratio is approximated analytically with the critical state model. A second model with a numerically optimized contour is developed in order to obtain a more accurate result. Both models can be applied to structures with moderate and large aspect ratios (10–10^4) that occur in newest generation of high-T_c tapes and coated conductors.

Based on the analysis of the shielding error in the contour approach and the difference in the results between the two methods it is concluded that the maximum error for the magnetization calculated with the optimized contour is better than 2% and in the analytical expression better than 5%.

The predicted magnetization loss in an ellipse is compared with experimental results on a high-T_c tape conductor with an aspect ratio of approximately 20. A good agreement is observed between the analytical model and the measurements in parallel and perpendicular magnetic fields if the filamentary zone is modeled as a single ellipse with fully coupled filaments.

The largest deviation between the experimental results for the AC loss of high-T_c tapes and the model for the ellipse occurs due to the field dependence of the critical current density. This deviation can be suppressed in the experiment by applying a background (DC) magnetic field on the tape.

The model calculations and the experimental results presented here do not agree with the model for an infinitely thin strip in a perpendicular field. The difference is attributed to the specific assumptions made to solve the thin strip model with an analytical method, in particular the constant critical current density distribution across the tape and the magnetic-field profile that does not exclude unsaturated currents in the shielded zone.

Acknowledgements

This research is supported by the Technology foundation STW, applied science division of NWO and the technology programme of the Ministry of Economic Affairs.

References

[1] C.P. Bean, Phys. Rev. Lett. 8 (1962) 250.
[2] E.H. Brandt, M.V. Indenbom, A. Forkl, Europhys. Lett. 22 (1993) 735.
[3] E. Zeldov, J.R. Clem, M. McElfresh, M. Darwin, Phys. Rev. B 49 (1994) 9802.
[4] M.N. Wilson, Superconducting Magnets, Clarendon Press, Oxford, 1983.
[5] J.V. Minervini, Adv. Cryo. Eng. 28 (1982) 587.
[6] K.V. Bhagwat, P. Chaddah, Physica C 254 (1995) 143.
[7] V.M. Krasnov, V.A. Larkin, V.V. Ryazanov, Physica C 174 (1991) 440.
[8] R. Navarro, L.J. Campbell, Phys. Rev. B 44 (1991) 10146.
[9] P.C. Rem, PhD thesis, University of Twente, Enschede, The Netherlands, 1986.
[10] R.A. Hartmann, PhD thesis, University of Twente, Enschede, The Netherlands, 1989.
[11] E.H. Brandt, Phys. Rev. B 54 (1996) 4246.
[12] N. Amemiya, K. Miyamoto, S. Murasawa, H. Mukai, K. Ohmatsu, Physica C 310 (1998) 30.
[13] J. Rhyner, Physica C 310 (1998) 42.
[14] T. Yazawa, J.J. Rabbers, B. ten Haken, H.H.J. ten Kate, H. Maeda, J. Appl. Phys. 84 (1998) 5652.
[15] P. Vase, R. Flükiger, M. Leghissa, B. Glowacki, Supercond. Sci. Technol. 13 (2000) 71.
[16] S.R. Foltyn et al., IEEE Trans. Appl. Supercond. 9 (1999) 1519.
[17] A.P. Malozemoff, S. Annavarapu, L. Fritzemeier, Q. Li, V. Prunier, M. Rupich, C. Thieme, W. Zhang, Inst. Phys. Conf. Ser. No. 167 (2000) 307.
[18] K. Kwasnitza, St. Clerc, Adv. Cryo. Eng. 40 (1994) 53.
[19] M.P. Oomen, J. Rieger, M. Leghissa, H.H.J. ten Kate, Appl. Phys. Lett. 70 (1997) 3038.
[20] J.J. Rabbers, O. van der Meer, W.F.A. Klein Zeggelink, O.A. Shevchenko, B. ten Haken, H.H.J. ten Kate, Physica C 325 (1999) 1.
[21] S.P. Ashworth, M. Suenaga, Physica C 313 (1999) 175.
[22] S.P. Ashworth, M. Maley, M. Suenaga, S.R. Foltyn, J.O. Willis, J. Appl. Phys. 88 (2000) 2718.
[23] J.J. Rabbers, B. ten Haken, H.H.J. ten Kate, Rev. Sci. Instr. 72 (2001) 2365.